Experimental Evidence for two Kinds of Defects in Amorphous $Fe_{80}B_{20}$ *

E. Nold, S. Steeb, and P. Lamparter

Max-Planck-Institut für Metallforschung, Institut für Werkstoffwissenschaften, Stuttgart, Germany

Z. Naturforsch. **35 a**, 610–612 (1980); received April 26, 1980

The scattering of cold neutrons ($\lambda = 1$ nm) with amorphous $Fe_{80}{}^{11}B_{20}$ yields a strong contribution at small $q = 4\pi \frac{\sin\Theta}{\lambda}$ $(0.07\,(\mathrm{nm})^{-1} \leq q \leq 2.4\,(\mathrm{nm})^{-1})$ arising from two kinds of defects of different size:

i) Local defects with an extent of about 1.5 nm,

ii) Extended defects with an extent of about 40 to 60 nm, which are interpreted as quasi-dislocations in the amorphous material.

Experimental Procedure and Results

Amorphous ribbons with the composition $Fe_{80}{}^{11}B_{20}$ were produced by melt spinning using as starting materials the Boron isotope ^{11}B together with iron of natural isotopic abundance for specimen A and with iron enriched in the ^{57}Fe-isotope for specimen B. The ribbons were cut to pieces of 25 mm length and packed together parallel to one another, thus forming a flat specimen $25 \times 8 \times 2\ \mathrm{mm}^3$. This specimen was orientated with its area perpendicular to the primary beam. By a cadmium frame placed before the specimen the irradiated area on the flat specimen was defined to $8 \times 8\ \mathrm{mm}^2$. Using these specimens, scattering experiments were performed at the cold source of the High Flux Reactor at the ILL, Grenoble using the small angle scattering apparatus D 17 working with slow neutrons ($\lambda = 1$ nm). Two arrangements of the counter were chosen: For larger q-values the distance specimen – counter amounted to 140 cm and the center of the counter was arranged at an angle of 10 degrees to the primary beam. For smaller q-values the distance specimen – counter amounted to 280 cm with the center of the counter being placed in the direction of the primary beam.

The measured intensities were corrected for background contribution and absorption. Concerning the scattering lengths and isotopic composition of the iron component in specimen A and B, respectively [1].

From the corrected intensities the coherent scattered intensity in absolute units was obtained by the method of the vanadium-calibration.

Figure 1 shows the differential cross section $(\mathrm{d}\sigma/\mathrm{d}\Omega)_{\mathrm{coh}}$ for coherent scattering versus $q = |\boldsymbol{q}| = 4\pi \frac{\sin\Theta}{\lambda}$ as obtained with specimen B. The scaling of the upper curve is different from that of the lower curve by a factor of 30.

Discussion

The curves in Fig. 1 show rather strong neutron scattering at small q-values, which normally is caused by one or more of the following effects, namely

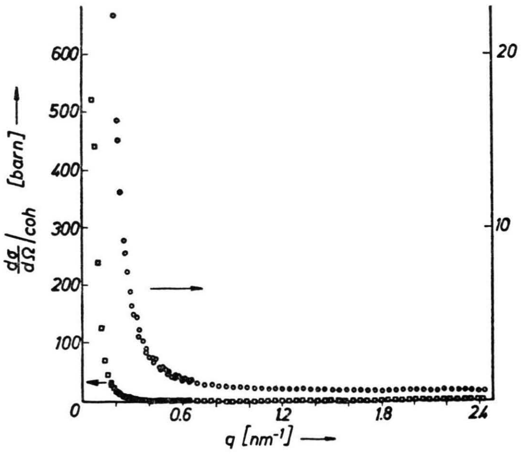

Fig. 1. $^{57}Fe_{80}{}^{11}B_{20}$: $(\mathrm{d}\sigma/\mathrm{d}\Omega)_{\mathrm{coh}}(q)$.

* The present paper is based on experiments which we kindly were allowed to perform at the high flux reactor of ILL, Grenoble.

Reprint requests to Prof. Dr. S. Steeb, Max-Planck-Institut für Metallforschung, Seestraße 92, 7000 Stuttgart 1.

0340-4811 / 80 / 0600-0610 \$ 01.00/0. — Please order a reprint rather than making your own copy.

magnetic scattering, scattering caused by concentration fluctuations, and scattering caused by density fluctuations.

i) Magnetic scattering

It should be stressed that the coherent differential cross section of Fig. 1 proved to be independent of the orientation of an applied external magnetic field H, which was orientated parallel to the length of the ribbons, however, once with $\boldsymbol{H}//\boldsymbol{q}$ and once with $\boldsymbol{H} \perp \boldsymbol{q}$. Also no influence of the strength of the external magnetic field which was varied between zero and 0.5 T could be recognized in the q-region of Fig. 1, namely for $0.07\ \mathrm{nm}^{-1} \leqq q \leqq 2.4\ \mathrm{nm}^{-1}$. From this fact we conclude the small angle scattering being caused by inhomogeneities of the nuclear scattering length density within the specimens and not by magnetic scattering. This conclusion is supported by X-ray small angle scattering experiments performed recently [2].

ii) Scattering from concentration fluctuations

Contributions to the scattered intensity which are caused by concentration fluctuations are proportional to the square of the difference (Δb) of the scattering lengths of the components. The comparison between $(\mathrm{d}\sigma/\mathrm{d}\Omega)_{\mathrm{coh}}$ as obtained from specimen A and from specimen B shows the same q-dependency. However, curve A lies below curve B in spite of the fact, that $(\Delta b)^2$ for specimen A is larger than for specimen B.

From this fact we conclude that the interpretation of the present experimental results is not possible in terms of concentration fluctuations.

iii) Scattering from density fluctuations

Based on the facts mentioned above, we discuss in the following the experimental results from Fig. 1 in terms of density fluctuations.

In Fig. 1 we observe below $q = 0.8\ \mathrm{nm}^{-1}$ a very strong rise towards $q \rightarrow 0$, for q larger than $1\ \mathrm{nm}^{-1}$ a rather flat run is observed. From this behaviour we conclude that the scattered intensity is caused by two kinds of defects of different size, which now will be discussed in detail.

Local Defects

From the q-region above $1\ \mathrm{nm}^{-1}$ in Fig. 1 we obtain a Guinier-plot as shown in Figure 2. This plot shows a linear run. From the gradient of the straight line a radius of gyration $R_g = 0.53$ nm was obtained. Recently a model of an amorphous monoatomic structure was generated by a computer simulation [3], which showed regions with a diameter of three to four atomic distances caused by internal short range stress [4].

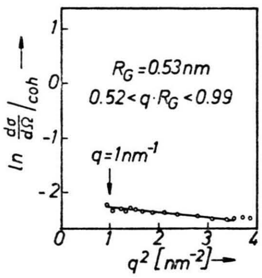

Fig. 2. $^{57}Fe_{80}{}^{11}B_{20}$: Guinier-plot ($q \geqq 1\ \mathrm{nm}^{-1}$) (arbitrary units).

Extended Defect Regions

From the q-region smaller than $0.6\ \mathrm{nm}^{-1}$ in Fig. 1 we obtain a Guinier-plot as shown in Figure 3. Since this plot shows no linear behaviour, the extrapolation method proposed by Guinier [5] was applied. During this method the gradient of the Guinier-plot vs. q^2 has to be extrapolated to $q^2 \rightarrow 0$ and yields a radius of gyration of about 27 nm.

Since the Guinier-plot shown in Fig. 3 didn't behave in a linear way, the model of diluted homogeneous particles does not hold.

Another possibility to yield an information concerning the extension of the extended defect regions consists in performing a Fourier transform.

In Fig. 4 we show the Fourier transform $G(r)$ which was obtained from $(\mathrm{d}\sigma/\mathrm{d}\Omega)_{\mathrm{coh}}(q)$ for q smaller than $0.62\ \mathrm{nm}^{-1}$. The $G(r)$ shows the radius of the extended defect regions being approximately 40 nm.

Figure 5 shows an alternative representation of the data, namely the plot $\log(\mathrm{d}\sigma/\mathrm{d}\Omega)_{\mathrm{coh}}$ vs. $\log q$.

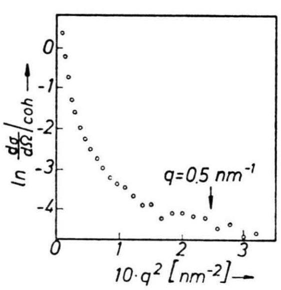

Fig. 3. $^{57}Fe_{80}{}^{11}B_{20}$: Guinier-plot ($q \leqq 0.6\ \mathrm{nm}^{-1}$) (arbitrary units).

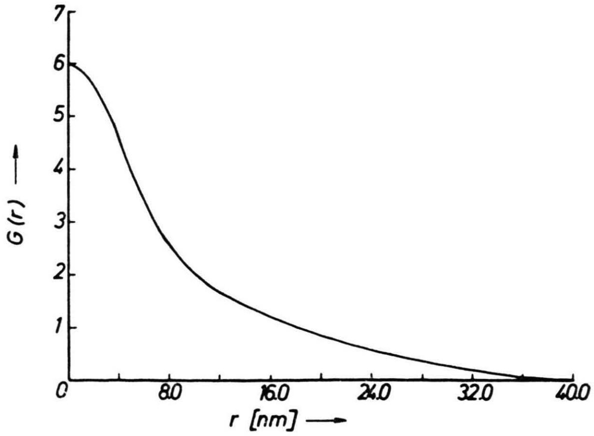

Fig. 4. $^{57}Fe_{80}{}^{11}B_{20}$: Fourier Transform of $(d\sigma/d\Omega)_{coh}(q)$ (arbitrary units).

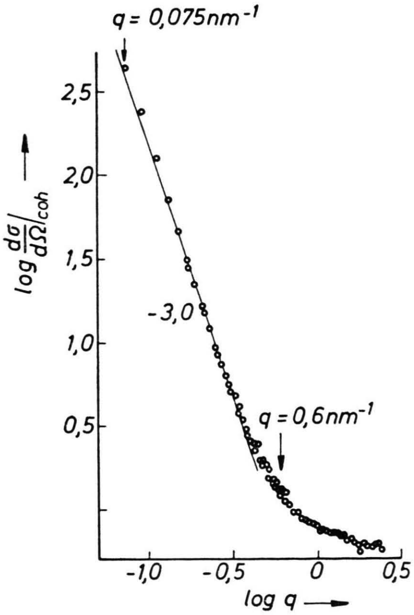

Fig. 5. $^{57}Fe_{80}{}^{11}B_{20}$: Double-logarithmic plot of $(d\sigma/d\Omega)_{coh}(q)$.

This plot shows linear behaviour in the region $0.075 \leqq q \leqq 0.6\ nm^{-1}$. The gradient of this straight line proves to be -3. This is according to Ref. [6] a strong hint on small angle scattering caused by edge dislocations. As a result we arrive at the following picture of the extended defect regions: They are regions with internal long range stress which behaves as the internal long range stress in crystals being caused by dislocations. Apparently the extended defect regions are produced by the rapid quenching process during the production of the amorphous ribbons: The non-uniformity of the solidification process within the ribbon leads to density fluctuations.

The fact already mentioned above, namely that specimen A yields larger $(d\sigma/d\Omega)_{coh}$-values than specimen B, easily can be understood by assuming different defect concentrations. For a quantitative treatment of the observed scattering effect it will be necessary to take into account also possible surface scattering (see for example [7]).

In Ref. [8] for the understanding of the magnetic behaviour of ferromagnetic amorphous materials it was necessary to claim the existence of quasi dislocation dipoles within these materials. According to Ref. [6] the SAS-intensity caused by dislocation dipoles behaves for $q > (1/d)$ (d = mean distance of the dislocations forming the dipole) according to q^{-3} and for $q < (1/d)$ according to q^{-1}. Since the lower q-limit of the present investigation amounts to $0.075\ nm^{-1}$ we would be only able to detect dipole scattering if the dipole distance would be smaller than 14 nm. At present we extend the measurements to lower q-values in order to study the q-dependency of the scattered intensity. This will allow to decide whether the extended defect regions are formed by single dislocations or quasi dislocation dipoles.

Acknowledgement

Thanks are due to the ILL, Grenoble, for allocation of beam time at the instrument D 17, the Deutsche Forschungsgemeinschaft, Bad Godesberg, for financial support, and to Dr. M. Wilkens for valuable discussions.

[1] M. Weber and S. Steeb, Z. Naturforsch. **33a**, 799 (1978).
[2] O. Kratky, Graz, private communication.
[3] T. Egami, K. Maeda, and V. Vitek, Phil. Mag. (1980) in press.
[4] T. Egami, private communication.
[5] A. Guinier and G. Fournet, Small Angle Scattering of X-Rays, John Wiley, New York 1955.
[6] H. H. Atkinson and P. B. Hirsch, Phil. Mag. **3**, 213 (1958).
[7] W. Schmatz, Riv. Nuovo Cim. **5**, 398 (1975).
[8] H. Kronmüller and J. Ulner, J. Magnetism Magnetic Mat. **6**, 52 (1977).